Title: FABP4 as a Therapeutic Host Target Controlling SARS-CoV2 Infection

Authors: Hatoon Baazim[1], Emre Koyuncu[2], Gürol Tuncman[1], M. Furkan Burak[1,13], Lea Merkel[1], Nadine Bahour[1], Ezgi Karabulut[1], Grace Yankun Lee[1], Alireza Hanifehnezhad[3], Zehra Firat Karagoz[4], Katalin Földes[5], Ilayda Engin[4], Ayse Gokce Erman[4], Sidika Oztop[3], Nazlican Filazi[6], Buket Gul[3], Ahmet Ceylan[7], Ozge Ozgenc Cinar[7], Fusun Can[8], Hahn Kim[2,9,10], Ali Al-Hakeem[2], Hui Li[11], Fatih Semerci[2], Xihong Lin[11], Erkan Yilmaz[4], Onder Ergonul[8], Aykut Ozkul[3*], & Gökhan S. Hotamisligil[1,12*]

Affiliations:

[1] Sabri Ülker Center for Metabolic Research, Dept. of Molecular Metabolism, Harvard T.H. Chan School of Public Health; Boston, MA, USA.

[2] Crescenta Biosciences Inc; Irvine, CA, USA.

[3] Ankara University, Faculty of Veterinary Medicine, Dept. of Virology; Ankara, Türkiye.

[4] Ankara University, Biotechnology Institute; Ankara, Türkiye.

[5] The Pirbright Institute, Ash Road, Pirbright, Woking GU24 0NF, UK

[6] Mustafa Kemal University, Faculty of Veterinary Medicine, Dept. of Virology; Hatay, Türkiye

[7] Ankara University, Faculty of Veterinary Medicine, Dept. of Histology and Embryology; Ankara, Türkiye

[8] Koç University, School of Medicine, Dept. of Infectious Diseases; Istanbul, Türkiye.

[9] Princeton University Small Molecule Screening Center, Princeton University; Princeton, NJ, USA.

[10] Dept. of Chemistry, Princeton University; Princeton, NJ, USA.

[11] Dept. of Biostatistics, Harvard T.H. Chan School of Public Health; Boston, MA, USA.

[12] Harvard-MIT Broad Institute; Cambridge, MA, USA

[13] Division of Endocrinology, Diabetes and Hypertension, Brigham and Women's Hospital, Harvard Medical School; Boston, MA, USA

*Corresponding author. Email: ghotamis@hsph.harvard.edu or Aykut.Ozkul@ankara.edu.tr

Abstract:

Host metabolic fitness is a critical determinant of infectious disease outcomes. In COVID-19, obesity and aging are major high-risk disease modifiers, although the underlying mechanism remains unknown. Here, we demonstrate that fatty acid binding protein 4 (FABP4), a critical regulator of metabolic dysfunction in these conditions, regulates SARS-CoV2 pathogenesis. Our study revealed that elevated FABP4 levels in COVID-19 patients strongly correlate with disease severity. In adipocytes and airway epithelial cells we found that loss of FABP4 function by genetic or pharmacological means impaired SARS-CoV2 replication and disrupted the formation of viral replication organelles. Furthermore, treatment of infected hamsters with FABP4 inhibitors alleviated lung damage and fibrosis and reduced lung viral titers. These results highlight a novel host factor critical for SARS-CoV2 infection and the therapeutic potential of FABP4-targeting agents in treating COVID-19 patients.

Introduction:

Viral infections are highly disruptive events that mobilize extensive resources to facilitate replication, organelle remodeling (*1*, *2*), and immune responses (*3*). The resulting immunometabolic interactions substantially modify the host's metabolic state, while also being greatly influenced by it (*4*). Though it is recognized that the host's metabolism is a critical determinant of infectious disease outcomes (*5–7*), a mechanistic understanding of how metabolism affects viral replication and pathogenesis remain limited. Along with age, obesity, and its associated metabolic pathologies, which share many immunometabolic underpinnings, strongly increase COVID-19-related morbidity and mortality (*6*, *8*). Earlier studies identified FABP4 as an exceptionally versatile regulator of energy resources (*9*, *10*) and a modulator of metabolic and inflammatory responses (*11*, *12*). While there is no known direct link between FABP4 and SARS-CoV2 infection, FABP4's role in promoting inflammation and metabolic dysfunction in several comorbidities that constitute high-risk COVID-19, including diabetes (*13*), cardiovascular disease (*14*), and airway disease (*11*, *12*). Adipose tissue dysfunction is another common element linking these comorbidities through its regulation of systemic metabolism, and its ability to secrete proinflammatory cytokines (*15*, *16*). Adipocytes are also permissible to SARS-CoV2 infection, as shown in cultured adipocytes (*17*, *18*). Furthermore, the detection of SARS-CoV2 RNA in the adipose tissue of deceased COVID-19 patients and infected animals (*17–20*) indicates that viral dissemination into the adipose tissue may occur naturally. Adipocytes are the most abundant source of FABP4 (*21*), and together with macrophages, endothelial and epithelial cells, present an overlapping target for SARS-CoV2 infection and FABP4 action. Finally, FABP4 is a critical regulator of intracellular lipid metabolism, composition and trafficking, processes that are essential for SARS-CoV2 infection (*22*, *23*). These observations prompted us to directly assess the impact of FABP4 in COVID-19.

In this study, we observed significantly elevated FABP4 levels in the serum and lungs of COVID-19 patients that highly correlate with disease severity. We then examined the intracellular interaction between FABP4 and SARS-CoV2 using cultured adipocytes, and bronchial epithelial cells. We demonstrated that, FABP4 is recruited to the double-membrane vesicles (DMVs) of virus replication organelles (ROs), which are membrane-bound compartments derived from remodeled cellular organelles (*1*, *2*). Pharmacological inhibition, or genetic deletion of FABP4 resulted in a significantly reduced viral titers, due to disrupted DMV numbers and organization. Importantly, FABP4 inhibition in infected hamsters significantly

reduced viral titers, and ameliorated lung damage and fibrosis. Together, these data indicate that FABP4 facilitates SARS-CoV2 infection and that therapeutic targeting of FABP4 may be a beneficial treatment strategy for mitigating COVID-19 severity and mortality in humans.

FABP4 protein levels correlate with disease severity in COVID-19 patients.

To assess FABP4's involvement in SARS-CoV-2 infection, we conducted immunohistochemical staining for FABP4 in lung biopsies obtained from individuals with COVID-19. This revealed a high FABP4 signal in the endothelial cells lining the small vessels of the lung parenchyma (Fig. 1A). We also examined circulating levels of FABP4 in two patient cohorts at distinct stages of disease severity according to WHO severity criteria (*24*) [Cohort 1 (table S2), November 2020 – May 2021, n=283, dominant variants: epsilon and alpha (*25*). Cohort 2 (table S3) March-May 2020, n=116, dominant variant: original Wuhan strain] and 45 healthy controls (table S1). (*26*) This analysis revealed a progressive increase in FABP4 levels in relation to the disease severity in both female and male subjects (Fig. 1, B and C, fig. S1D). We further interrogated this relation by analyzing FABP4 concentration over time in each patient, adjusting for age, sex, and BMI. This confirmed the significance of the increase in FABP4 in severe and critical irrespective of those variables (Fig. 1D). Additionally, this pattern corresponded with an increase in several biomarkers of disease severity, including IL-6, C-reactive protein and circulating leukocytes (Fig. 1E, fig. S1, A, B and E). In critically ill patients, the percentage of circulating lymphocytes was reduced (fig. S1C). We then examined FABP4 levels in severe and critically ill patients in relation to BMI, age, and comorbidities. We found that FABP4 levels were only significant in patients with a BMI over 30 in our second cohort and were slightly elevated in the first cohort (Fig. 1F, fig. S1F). On the other hand, we found that patients over 50 years of age and those with comorbidities had significantly higher FABP4 levels (Fig. 1, F and G, fig. S1, G and H). Taken together, these data point to a strong regulation and potential involvement of FABP4 in the pathophysiology of SARS-CoV2 and suggests that the presence of underlying conditions that are regulated by FABP4 could further influence its involvement.

SARS-CoV2 infection is accelerated in mature adipocytes.

Due to the central role of adipocytes in aging and obesity-related metabolic dysfunction, and their high FABP4 abundance (*21*), we investigated the dynamics of SARS-CoV2 infection in the human Telomerase Reverse Transcriptase (hTERT) immortalized preadipocyte cell line (*26*). Preadipocytes and mature adipocytes were infected with SARS-CoV2 (WA1/2020, MOI 0.1 or 1). Though the nucleocapsid RNA was seemingly unchanged over time (Fig.2A), its protein abundance increased (fig. S2, C, E and G). Infected adipocytes also increased IL-6 secretion (fig. S2A). Interestingly, viral propagation was significantly higher in mature adipocytes, most notably, in viral titers, which exceeded that of preadipocytes by two orders of magnitude (Fig. 2, A to C). Infection of adipocytes at various stages of differentiation revealed a striking gradual increase in viral replication over the course of adipocyte maturation as evident by the increased virus titers and nucleocapsid protein abundance (Fig. 2, D to F). As expected, FABP4 abundance also increased during adipocyte differentiation (*27*) (Fig. 2, E and F).

We examined the morphology of infected mature adipocytes and found that nucleocapsid-positive cells contained significantly smaller lipid droplets (LDs) compared to neighboring cells (Fig. 2, G and H), suggesting a depletion in infected cells' lipid stores. Staining of the ER membrane protein calnexin, revealed a change in its distribution in infected cells (Fig. 2I), where

it condensed, forming puncti that co-localized with viral dsRNA (Fig. 2K), a pattern that is indicative of DMVs (*28*). These results confirm that hTERT cells provide a good model to study SARS-CoV2 infection in human adipocytes and suggest that SARS-CoV2 replication is accelerated in cells of a higher lipid content.

SARS-CoV2 infection recruits FABP4 to virus replication organelles.

To contextualize the role of intracellular FABP4 during infection, we examined its expression, protein abundance and secretion (fig. S2, B to D). In this setting, FABP4 levels were similar across samples collected at 24 and 48 hours after infection. Fluorescence staining revealed a striking change in their spatial distribution of FABP4 within infected cells (Fig. 2, J and K, fig. S2F). In dsRNA positive cells, FABP4 condensed into puncti that co-localized with the dsRNA signal (Fig. 2, J and K). Whereas in nucleocapsid positive cells, the FABP4 signal was distributed across the cytoplasm (fig. S2F). Both patterns were observed in neighboring cells, suggesting a dynamic change in FABP4 distribution at different stages of infection (fig. S2F). These data show that FABP4 is recruited to the ROs and may play a role in virus replication.

FABP4 deficiency impairs coronavirus replication.

To understand the functional relevance of FABP4 in SARS-CoV2 infection, we utilized small molecule inhibitors of FABP4. For these experiments, we used two structurally different inhibitors targeting FABP4: the previously established BMS309403 (*30*) and CRE-14, which represents a newly developed class of FABP inhibitors (*31*). We validated and confirmed the activity of these molecules in competing with FABP4 ligands using the Terbium-based time-resolved fluorescence energy transfer assay (TR-FRET). We confirmed that both BMS309403 and CRE-14 were able to block FABP4's ability to bind its lipid ligands (BODIPY FL C12) (fig. S3C). Using a micro-scale thermophoresis (MST) assay, we determined that CRE-14 binds FABP4 with a (K_D = 954nM) (fig. S3A and B).

Mature human adipocytes were treated with FABP4 inhibitors following SARS-CoV2 infection (MOI 0.1 or 1). This inhibition significantly reduced virus nucleocapsid RNA and protein levels and resulted in a remarkable reduction in the virus titers (Fig. 3, A to F, fig. S3, F and G). IL-6 secretion in the inhibitor treated cells was significantly lower 48 hours post-infection (fig. S3E), indicating an ameliorated inflammatory state. We then infected mature adipocytes with a higher viral dose (MOI 3) to increase the incidence of dsRNA-positive cells, and thereby enable a better quantitative characterization of the dsRNA puncti. Interestingly, the dsRNA puncti in the FABP4-inhibitor treated samples appeared scattered across the cytoplasm failing to form coherent clusters (Fig. 3G), suggesting disruption of DMV formation in which they are packed. A quantitative evaluation of the dsRNA positive signal in the confocal images showed a significant reduction in the percentage of dsRNA-positive area and mean fluorescence intensity per cell (fig. 3H), which confirmed the observed disruption in DMV formation.

To further confirm the relevance of FABP4 in SARS-CoV2 replication in a genetic model, we generated FABP4-deficient human adipocyte cell lines through CRISPR-mediated deletion as well as shRNA suppression. In both models, viral titers were significantly reduced in the absence of FABP4 (Fig. 3I, fig. S3H), which was also reflected in the reduced nucleocapsid protein in the FABP4 knockout cells (Fig. 3, J and K).

These data demonstrated the critical importance of FABP4 for SARS-CoV2 replication, likely through its engagement with the DMVs in the ROs. We also examined the relevance of FABP4 for the common cold coronavirus (OC43) infection using a Real-Time Cell Electronic Sensing assay (RTCES) to measure cell viability and cytopathic effects (CPE) in wild type and FABP4 knockout mouse pre-adipocytes (fig. S3, I and J), as well as human lung fibroblasts (MRC5) treated with the FABP4 inhibitor CRE-14 (fig. S3K) and observed a significant delay in virus-induced CPE in the absence of FABP4 function, confirming the relevance of FABP4 in other coronaviruses.

FABP4 facilitates virus replication in bronchial epithelial cells.

Having established FABP4's significance in SARS-CoV2 adipocyte infection, we investigated its role in human bronchial epithelial (HBE) cells to understand whether it is engaged early on during respiratory tract infection (*32*). HBE135-E6E7 cells were infected with high titers (MOI 5) of various isolates of SARS-CoV2 representing the alpha, delta, omicron, and Eris variants (Ank1, Ank-Dlt1, and Ank-Omicron GKS, Ank-Eris respectively). Following infection, cells were treated with two doses of FABP4 inhibitors, and their viral titers (measured as $TCID_{50}$) were monitored over four days (Fig. 4, A and B, fig. S4, A to F). In all tested conditions, FABP4 inhibition resulted in a marked reduction of virus titers. Next, we used transmission electron microscopy (TEM) to examine the consequence of FABP4 inhibition on ROs morphology. Infected HBE cells (MOI 1) were treated with the FABP4 inhibitor (CRE-14) then fixed 48 hours post-infection. TEM imaging revealed a marked reduction in the size of DMVs following FABP4 inhibitor treatment (Fig. 4, C and D).

We also utilized reconstructed airway epithelium organoids that were apically infected with SARS-CoV2 and treated with either 1.1μM or 10μM CRE-14 or 5μM of the antiviral Remdesivir through the basal layer. Viral titers measured from the apical wash showed a reduction following inhibitor treatment 72 hours post-infection that, at the higher dose, matched the titers of the Remdesivir treated group (Fig.4E). We then examined the morphology and distribution of DMVs in the vehicle or 10μM CRE-14 treated organoids and observed that in the inhibitor-treated group DMVs were reduced in both size and numbers (Fig. 4, F, H and I) and appeared more dispersed, failing to form the tight clusters observed in untreated controls (Fig. 4J). Clusters of LDs were observed in infected samples and were nearly absent in the inhibitor-treated group (Fig. 4G). Importantly, we confirmed that exposure to FABP4 inhibitor in uninfected samples did not alter cellular or organelle morphology (fig. S4G). We performed a similar analysis in samples treated with the BMS309403 compound, and though we observed similar results, the phenotype was less pronounced, and the compound treatment induced a significant degree of cell death in the organoids (fig. S4, H to J). Overall, these data confirm the importance of FABP4 for SARS-CoV2 replication through its influence on the ROs formation in multiple cellular targets. Its engagement with virus infection in airway epithelial cells and adipocytes, also increases its potential as a therapeutic target.

FABP4 inhibition reduces viral titer and lung damage in infected hamsters.

To examine the therapeutic potential of FABP4 inhibitor treatment in a preclinical model *in vivo*, we infected 12–14-week-old lean Syrian hamsters with SARS-CoV2 (Ank1, 100 $TCID_{50}$) (*33*), and treated them for 6-days with a subcutaneous injection of 15 mg/kg FABP4 inhibitor BMS309403 and CRE-14 or vehicle (Fig. 5, fig. S5). The hamsters were monitored daily, and the experiments were terminated for virus titer measurements (right lung) and histological

analysis (left lung). Inhibitor treatment significantly ameliorated the infection-associated weight loss (Fig. 5A), and the viral titers were consistently decreased upon treatment with FABP4 inhibitor (Fig. 5B).

We further examined the effect of FABP4 inhibition on lung pathology and observed a notable reduction in lung damage in H&E-stained samples (Fig. 5C). Quantification of these histology images revealed a significant reduction in the percentage of damaged lung tissue (Fig. 5D) and an improvement in alveolar space (Fig. 5E) indicating a lower degree of alveolar collapse. Trichrome staining revealed an increase collagen deposition in the lung following infection which was reduced with inhibitor treatment (Fig.5G). Moreover, immunohistochemical staining for the SARS-CoV2 nucleocapsid protein revealed that the nucleocapsid positive areas were reduced both in number and in size after inhibitor treatment (Fig. 5, F, H and I). Hamster treatment with BMS309403 resulted in similar but less pronounced results (fig. S5, D and E). This might be explained in part by the higher plasma exposure and better pharmacokinetics of CRE-14 as assessed in mice (fig. S5 A to C).

Discussion:

In this study, we observed a striking elevation in circulating FABP4 levels in COVID-19 patients, correlating with disease severity at a level comparable to the most established clinical biomarker IL-6. Using *in vitro* studies, we demonstrated the significant impact of FABP4 on SARS-CoV2 replication in multiple cellular targets using chemical and genetic interventions and multiple strains of the virus. We also demonstrated the relevance of FABP4 activity in an *in vivo* infection model of Syrian hamsters, where targeting FABP4 with small molecule inhibitors significantly reduced the viral titers in the lungs and alleviated overall lung damage and fibrosis. Taken together, our data demonstrates FABP4 as a novel host factor that is critical for SARS-CoV2 infection, targeting of which may offer unique opportunities for disease management.

FABP4 has a marked impact on the pathogenesis of metabolic diseases associated with obesity and aging (*34*). Interestingly, FABP4 levels are also increased in obese mice and humans and correlate positively with cardiometabolic pathologies and morbidity (*35*). Furthermore, humans carrying a low-expression variant of FABP4 exhibit significant protection against the development of type 2 diabetes and cardiometabolic disease in multiple GWAS studies (*36*). As such, the impact of targeting FABP4 on overall pathogenesis of COVID-19 may not be limited to reduced viral titers. FABP4 can also influence the inflammatory and metabolic milieu both with in the local environment of the lungs, and systemically as its effects extend across metabolic organs. Consequently, targeting FABP4 may result in improvements of cardiometabolic as well as pulmonary fitness and protection against potential tissue damage and long-term consequences of SARS-CoV2 infection in humans. While this requires further investigation, the reduction in lung damage and fibrosis that we observed in our inhibitor-treated, SARS-CoV2-infected hamsters does highlight this possibility, particularly pertaining to the mitigation of respiratory symptoms associated with long-COVID (*37*).

Remodeling of host intracellular membranes into virus replication organelles (ROs) is a strategy used by Coronaviruses and other positive stranded RNA (+RNA) viruses, to support their propagation and secretion and provide an environment shielded from immune recognition (*2, 38*). In the case of coronaviruses, these compartments consist of DMVs, spherules, and zippering ER membranes. In this study, we observed a striking recruitment of FABP4 to ROs in infected cells. The FABP4 signal, which is usually diffused throughout the cytoplasm, condensed into puncti colocalized with dsRNA signals, pointing to their recruitment to DMVs. Examination

of infected adipocytes and bronchial epithelial cells with confocal microscopy and TEM revealed that the DMVs in cells where FABP4 was inhibited were smaller and more dispersed. We suggest that this loss of a spatial organization of the DMVs is what resulted in the reduced viral replication capacity, evident by the lower virus nucleocapsid RNA and protein, and overall viral titers. How FABP4 contributes to the formation of ROs will be an interesting future question to explore as this may open new potential points of intervention to viral replication. For example, FABP4 can influence *de novo* lipogenesis and lipid droplet formation, as well as lipid composition in the context of metabolic diseases or directly influence lipid substrate supply for RO biogenesis (*39*, *40*). Therefore, by facilitating changes in the lipid landscape, FABP4 may impact the subcellular architectural remolding required for RO generation (*41–43*). In fact, in this study, we demonstrate that human adipocytes' capacity for virus replication increased as they matured. These observations might provide one possible explanation of how obesity can exacerbate disease severity in COVID-19, both due to the higher lipid content in adipocytes and the ectopic lipid deposition at other organs associated with obesity (*39*).

In summary, our works demonstrates a critical contribution of FABP4 to SARS-CoV2 virus replication, and highlights FABP4 as a therapeutic target acting both as an antiviral and a modulator of cardio-pulmonary and metabolic fitness.

References and Notes

1. M. Cortese, J.-Y. Lee, B. Cerikan, C. J. Neufeldt, V. M. J. Oorschot, S. Köhrer, J. Hennies, N. L. Schieber, P. Ronchi, G. Mizzon, I. R. Brey, R. Santarella-Mellwig, M. Schorb, M. Boermel, K. Mocaer, M. S. Beckwith, R. M. Templin, V. Gross, J. Frankish, N. K. Horvat, V. Laketa, M. Stanifer, S. Boulant, A. Ruggieri, L. Chatel-Chaix, Y. Schwab, R. Bartenschlager, Integrative Imaging Reveals SARS-CoV-2 Induced Reshaping of Subcellular Morphologies. *Cell Host Microbe*, doi: 10.2139/ssrn.3668344 (2020).
2. P. Roingeard, S. Eymieux, J. Burlaud-Gaillard, C. Hourioux, R. Patient, E. Blanchard, The double-membrane vesicle (DMV): a virus-induced organelle dedicated to the replication of SARS-CoV-2 and other positive-sense single-stranded RNA viruses. *Cellular and Molecular Life Sciences* **79**, 1–9 (2022).
3. M. S. Diamond, T. D. Kanneganti, Innate immunity: the first line of defense against SARS-CoV-2. *Nat Immunol* **23**, 165–176 (2022).
4. A. Lercher, H. Baazim, A. Bergthaler, Systemic Immunometabolism: Challenges and Opportunities. *Immunity* **53**, 496–509 (2020).
5. N. Stefan, A. L. Birkenfeld, M. B. Schulze, Global pandemics interconnected — obesity, impaired metabolic health and COVID-19. *Nat Rev Endocrinol* **17**, 135–149 (2021).
6. X. Fan, J. Han, E. Zhao, J. Fang, D. Wang, Y. Cheng, Y. Shi, Z. Wang, Z. Yao, P. Lu, T. Liu, Q. Li, K. L. Poulsen, Z. Yuan, Y. Song, J. Zhao, The effects of obesity and metabolic abnormalities on severe COVID-19-related outcomes after vaccination: A population-based study. *Cell Metab* **35**, 585-600.e5 (2023).
7. R. Honce, S. Schultz-Cherry, Impact of obesity on influenza A virus pathogenesis, immune respoanse, and evolution. Frontiers Media S.A. [Preprint] (2019). https://doi.org/10.3389/fimmu.2019.01071.
8. N. Stefan, A. L. Birkenfeld, M. B. Schulze, Global pandemics interconnected — obesity, impaired metabolic health and COVID-19. *Nat Rev Endocrinol* **17**, 135–149 (2021).
9. K. J. Prentice, J. Saksi, G. S. Hotamisligil, Adipokine FABP4 integrates energy stores and counterregulatory metabolic responses. *J Lipid Res* **60**, 734–740 (2019).
10. K. J. Prentice, J. Saksi, L. T. Robertson, G. Y. Lee, K. E. Inouye, K. Eguchi, A. Lee, O. Cakici, E. Otterbeck, P. Cedillo, P. Achenbach, A. G. Ziegler, E. S. Calay, F. Engin, G. S. Hotamisligil, A hormone complex of FABP4 and nucleoside kinases regulates islet function. *Nature* **600**, 720–726 (2021).
11. B. O. V. Shum, C. R. Mackay, C. Z. Gorgun, M. J. Frost, R. K. Kumar, G. S. Hotamisligil, M. S. Rolph, The adipocyte fatty acid-binding protein aP2 is required in allergic airway inflammation. *J Clin Invest* **116**, 2183–2192 (2006).
12. X. N. Ge, I. Bastan, M. Dileepan, Y. Greenberg, S. G. Ha, K. A. Steen, D. A. Bernlohr, S. P. Rao, P. Sriramarao, FABP4 regulates eosinophil recruitment and activation in allergic airway inflammation. *Am J Physiol Lung Cell Mol Physiol* **315**, L227–L240 (2018).

13. K. J. Prentice, J. Saksi, L. T. Robertson, G. Y. Lee, K. E. Inouye, K. Eguchi, A. Lee, O. Cakici, E. Otterbeck, P. Cedillo, P. Achenbach, A. G. Ziegler, E. S. Calay, F. Engin, G. S. Hotamisligil, A hormone complex of FABP4 and nucleoside kinases regulates islet function. *Nature* **600**, 720–726 (2021).
14. E. Erbay, V. R. Babaev, J. R. Mayers, L. Makowski, K. N. Charles, M. E. Snitow, S. Fazio, M. M. Wiest, S. M. Watkins, M. F. Linton, G. S. Hotamisligil, Reducing endoplasmic reticulum stress through a macrophage lipid chaperone alleviates atherosclerosis. *Nat Med* **15**, 1383–1391 (2009).
15. M.-Y. Ou, H. Zhang, P.-C. Tan, S.-B. Zhou, Q.-F. Li, Adipose tissue aging: mechanisms and therapeutic implications. doi: 10.1038/s41419-022-04752-6.
16. C. R. Kahn, G. Wang, K. Y. Lee, Altered adipose tissue and adipocyte function in the pathogenesis of metabolic syndrome. American Society for Clinical Investigation [Preprint] (2019). https://doi.org/10.1172/JCI129187.
17. M. Zickler, S. Stanelle-Bertram, S. Ehret, F. Heinrich, P. Lange, B. Schaumburg, N. M. Kouassi, S. Beck, M. Y. Jaeckstein, O. Mann, S. Krasemann, M. Schroeder, D. Jarczak, A. Nierhaus, S. Kluge, M. Peschka, H. Schlüter, T. Renné, K. Pueschel, A. Kloetgen, L. Scheja, B. Ondruschka, J. Heeren, G. Gabriel, Replication of SARS-CoV-2 in adipose tissue determines organ and systemic lipid metabolism in hamsters and humans. [Preprint] (2022). https://doi.org/10.1016/j.cmet.2021.12.002.
18. T. D. Saccon, F. Mousovich-Neto, R. G. Ludwig, V. C. Carregari, A. B. dos Anjos Souza, A. S. C. dos Passos, M. C. Martini, P. P. Barbosa, G. F. de Souza, S. P. Muraro, J. Forato, M. R. Amorim, R. E. Marques, F. P. Veras, E. Barreto, T. T. Gonçalves, I. M. Paiva, N. P. B. Fazolini, C. M. K. Onodera, R. B. Martins Junior, P. H. C. de Araújo, S. S. Batah, R. M. M. Viana, D. M. de Melo, A. T. Fabro, E. Arruda, F. Queiroz Cunha, T. M. Cunha, M. A. M. Pretti, B. J. Smith, H. Marques-Souza, T. L. Knittel, G. P. Ruiz, G. S. Profeta, T. C. M. Fontes-Cal, M. Boroni, M. A. R. Vinolo, A. S. Farias, P. M. M. Moraes-Vieira, J. M. A. Bizzacchi, T. Teesalu, F. D. M. Chaim, E. Cazzo, E. A. Chaim, J. L. Proença-Módena, D. Martins-de-Souza, M. K. Osako, L. O. Leiria, M. A. Mori, SARS-CoV-2 infects adipose tissue in a fat depot- and viral lineage-dependent manner. *Nat Commun* **13**, 1–15 (2022).
19. M. Reiterer, M. Rajan, N. Gómez-Banoy, J. D. Lau, L. G. Gomez-Escobar, L. Ma, A. Gilani, S. Alvarez-Mulett, E. T. Sholle, V. Chandar, Y. Bram, K. Hoffman, P. Bhardwaj, P. Piloco, A. Rubio-Navarro, S. Uhl, L. Carrau, S. Houhgton, D. Redmond, A. P. Shukla, P. Goyal, K. A. Brown, B. R. tenOever, L. C. Alonso, R. E. Schwartz, E. J. Schenck, M. M. Safford, J. C. Lo, Hyperglycemia in acute COVID-19 is characterized by insulin resistance and adipose tissue infectivity by SARS-CoV-2. *Cell Metab* **33**, 2174-2188.e5 (2021).
20. G. J. Martínez-Colón, K. Ratnasiri, H. Chen, S. Jiang, E. Zanley, A. Rustagi, R. Verma, H. Chen, J. R. Andrews, K. D. Mertz, A. Tzankov, D. Azagury, J. Boyd, G. P. Nolan, C. M. Schürch, M. S. Matter, C. A. Blish, T. L. McLaughlin, SARS-CoV-2 infection drives an inflammatory response in human adipose tissue through infection of adipocytes and macrophages. *Sci Transl Med* **14** (2022).
21. V. Matarese, D. A. Bernlohr, Purification of murine adipocyte lipid-binding protein. Characterization as a fatty acid- and retinoic acid-binding protein. *Journal of Biological Chemistry* **263**, 14544–14551 (1988).
22. K. N. Theken, S. Y. Tang, S. Sengupta, G. A. FitzGerald, The roles of lipids in SARS-CoV-2 viral replication and the host immune response. [Preprint] (2021). https://doi.org/10.1016/J.JLR.2021.100129.
23. S. da Silva Gomes Dias, V. C. Soares, A. C. Ferreira, C. Q. Sacramento, N. Fintelman-Rodrigues, J. R. Temerozo, L. Teixeira, M. A. N. da Silva, E. Barreto, M. Mattos, C. S. de Freitas, I. G. Azevedo-Quintanilha, P. P. A. Manso, M. D. Miranda, M. M. Siqueira, E. D. Hottz, C. R. R. Pão, D. C. Bou-Habib, D. F. Barreto-Vieira, F. A. Bozza, T. M. L. Souza, P. T. Bozza, Lipid droplets fuel SARS-CoV-2 replication and production of inflammatory mediators. *PLoS Pathog* **16**, e1009127 (2020).
24. World Health Organization, COVID-19 Clinical management. (2021).
25. T. P. Peacock, R. Penrice-Randal, J. A. Hiscox, W. S. Barclay, SARS-CoV-2 one year on: evidence for ongoing viral adaptation. *J Gen Virol* **102** (2021).
26. K. M. Lee, K. H. Choi, M. M. Ouellette, Use of exogenous hTERT to immortalize primary human cells. *Cytotechnology* **45**, 33–38 (2004).
27. I. Schlottmann, M. Ehrhart-Bornstein, M. Wabitsch, S. R. Bornstein, V. Lamounier-Zepter, Calcium-dependent release of adipocyte fatty acid binding protein from human adipocytes. *Int J Obes* **38**, 1221–1227 (2014).
28. T. Hackstadt, A. I. Chiramel, F. H. Hoyt, B. N. Williamson, C. A. Dooley, P. A. Beare, E. de Wit, S. M. Best, E. R. Fischer, Disruption of the golgi apparatus and contribution of the endoplasmic reticulum to the sars-cov-2 replication complex. *Viruses* **13**, 1798 (2021).
29. M. R. A. A. Syamsunarno, T. Iso, H. Hanaoka, A. Yamaguchi, M. Obokata, N. Koitabashi, K. Goto, T. Hishiki, Y. Nagahata, H. Matsui, M. Sano, M. Kobayashi, O. Kikuchi, T. Sasaki, K. Maeda, M. Murakami, T. Kitamura, M. Suematsu, Y. Tsushima, K. Endo, G. S. Hotamisligil, M. Kurabayashi, A critical role of

fatty acid binding protein 4 and 5 (FABP4/5) in the systemic response to fasting. *PLoS One* **8**, e79386 (2013).
30. M. Furuhashi, G. Tuncman, C. Z. Görgün, L. Makowski, G. Atsumi, E. Vaillancourt, K. Kono, V. R. Babaev, S. Fazio, M. F. Linton, R. Sulsky, J. A. Robl, R. A. Parker, G. S. Hotamisligil, Treatment of diabetes and atherosclerosis by inhibiting fatty-acid-binding protein aP2. *Nature 2007 447:7147* **447**, 959–965 (2007).
31. Emre. Koyuncu, Hahn. Kim, G. S. Hotamisligil, Novel cell metabolism modulating compounds and uses thereof for the treatment of viral diseases - US Patent Application 17/566692 (2023).
32. G. Beucher, M. L. Blondot, A. Celle, N. Pied, P. Recordon-Pinson, P. Esteves, M. Faure, M. Métifiot, S. Lacomme, D. Dacheux, D. R. Robinson, G. Längst, F. Beaufils, M. E. Lafon, P. Berger, M. Landry, D. Malvy, T. Trian, M. L. Andreola, H. Wodrich, Bronchial epithelia from adults and children: SARS-CoV-2 spread via syncytia formation and type III interferon infectivity restriction. *Proc Natl Acad Sci U S A* **119** (2022).
33. A. Hanifehnezhad, E. Ş. Kehribar, S. Öztop, A. Sheraz, S. Kasırga, K. Ergünay, S. Önder, E. Yılmaz, D. Engin, T. Ç. Oğuzoğlu, U. Ö. Ş. Şeker, E. Yılmaz, A. Özkul, Characterization of local SARS-CoV-2 isolatesand pathogenicity in IFNAR−/- mice. *Heliyon* **6** (2020).
34. K. N. Charles, M.-D. Li, F. Engin, A. P. Arruda, K. Inouye, G. S. Hotamisligil, Uncoupling of metabolic health from longevity through genetic alteration of adipose tissue lipid-ninding proteins. *Cell Rep* **21**, 393–402 (2017).
35. K. J. Prentice, J. Saksi, G. S. Hotamisligil, Adipokine FABP4 integrates energy stores and counterregulatory metabolic responses. *J Lipid Res* **60**, 734–740 (2019).
36. E. H. Dahlström, J. Saksi, C. Forsblom, N. Uglebjerg, N. Mars, L. M. Thorn, V. Harjutsalo, P. Rossing, T. S. Ahluwalia, P. J. Lindsberg, N. Sandholm, P. H. Groop, The low-expression variant of FABP4 is associated with cardiovascular disease in type 1 diabetes. *Diabetes* **70**, 2391–2401 (2021).
37. H. E. Davis, L. McCorkell, J. M. Vogel, E. J. Topol, Long COVID: major findings, mechanisms and recommendations. *Nat Rev Microbiol* **21**, 133–146 (2023).
38. G. Wolff, C. E. Melia, E. J. Snijder, M. Bárcena, Double-membrane vesicles as platforms for viral replication. *Trends Microbiol* **28**, 1022–1033 (2020).
39. K. Maeda, H. Cao, K. Kono, C. Z. Gorgun, M. Furuhashi, K. T. Uysal, Q. Cao, G. Atsumi, H. Malone, B. Krishnan, Y. Minokoshi, B. B. Kahn, R. A. Parker, G. S. Hotamisligil, Adipocyte/macrophage fatty acid binding proteins control integrated metabolic responses in obesity and diabetes. *Cell Metab* **1**, 107–119 (2005).
40. N.-S. Tan, N. S. Shaw, N. Vinckenbosch, P. Liu, R. Yasmin, B. Desvergne, W. Wahli, N. Noy, Selective cooperation between fatty acid binding proteins and peroxisome proliferator-activated receptors in regulating transcription. *Mol Cell Biol* **22**, 5114–5127 (2002).
41. S. da Silva Gomes Dias, V. C. Soares, A. C. Ferreira, C. Q. Sacramento, N. Fintelman-Rodrigues, J. R. Temerozo, L. Teixeira, M. A. N. da Silva, E. Barreto, M. Mattos, C. S. de Freitas, I. G. Azevedo-Quintanilha, P. P. A. Manso, M. D. Miranda, M. M. Siqueira, E. D. Hottz, C. R. R. Pão, D. C. Bou-Habib, D. F. Barreto-Vieira, F. A. Bozza, T. M. L. Souza, P. T. Bozza, Lipid droplets fuel SARS-CoV-2 replication and production of inflammatory mediators. *PLoS Pathog* **16**, e1009127 (2020).
42. C. G. Williams, A. S. Jureka, J. A. Silvas, A. M. Nicolini, S. A. Chvatal, J. Carlson-Stevermer, J. Oki, K. Holden, C. F. Basler, Inhibitors of VPS34 and fatty-acid metabolism suppress SARS-CoV-2 replication. *Cell Rep* **36**, 109479 (2021).
43. S. Ricciardi, A. M. Guarino, L. Giaquinto, E. V. Polishchuk, M. Santoro, G. Di Tullio, C. Wilson, F. Panariello, V. C. Soares, S. S. G. Dias, J. C. Santos, T. M. L. Souza, G. Fusco, M. Viscardi, S. Brandi, P. T. Bozza, R. S. Polishchuk, R. Venditti, M. A. De Matteis, The role of NSP6 in the biogenesis of the SARS-CoV-2 replication organelle. *Nature* **606**, 761–768 (2022).

Acknowledgments: We thank all members of the Hotamisligil Laboratory, past and present, for their scientific support and input during the development of this project. We also thank Drs. Phyllis Kanki, and Don Hamel for their support in facilitating our work in the BSL-3 facility at Harvard Chan School, Dr. Lynn Enquist of Princeton University for his valuable feedback, Dr. Pinar Firat from Koç University and Dr. Nur Urer from the Ministry of Health Yedikule State Hospital for help with human histological samples. Electron microscopy image analysis was

conducted with assistance from the Image Analysis Collaboratory at Harvard Medical School (https://iac.hms.harvard.edu/).

Funding: Support by Hotamisligil Lab and Crescenta Biosciences for their part of the experiments.

Author contributions: HB designed and performed the *in vitro* experiments and analyzed the data, performed the histology, fluorescence, and electron microscopy image analysis, prepared the figures, and wrote and revised the manuscript. EK designed, supervised, and performed experiments relating to the CRE-14 compound and OC43 virus infection, interpreted results, revised the manuscript, and contributed to the conception of the project. GT and FB provided intellectual contributions and coordinated collaborations. HK designed and synthesized the CRE-14 compound and provided intellectual contributions and contributed to the conception of the project. LM generated the human FABP4 knockout cell lines and together with NB performed sample analysis. GYL provided intellectual insight and assistance in generating the human FABP4 knockout cell lines. AH and ZFK performed *in vivo* hamster experiments. NF, and BG performed *in vitro* assays and analyzed data. SO, AC, OOC, and FS performed histological sample preparations and analyzed the data. AA Established the RTCES assay protocols and analyzed data. EY, IE and AGE maintained the animal colonies and designed and prepared animal cohorts and supervised animal experiments. FC and ÖE conducted all human studies and performed the FABP4 measurements in human samples. HL and XL performed the statistical analysis for the human data. AÖ planned, supervised, and conducted all hamster infection experiments and analysis of the results and revised the manuscript. GSH conceived, supervised and supported the project, designed experiments, interpreted results and planned and revised the manuscript.

Competing interests: EK is co-founder, director and officer of Crescenta Biosciences and holds equity at the company. AA and FS are employees of Crescenta Biosciences. HK is co-founder, director, and consultant of Crescenta Biosciences and holds equity at the company. HK is an employee of Princeton University; All work of HK included herein was performed as a consultant for Crescenta, independent of Princeton University. HK, EK and GSH are inventors on patent application that includes CRE-14. GSH is a scientific advisor, receives compensation and holds equity at Crescenta Biosciences. Other authors declare no competing interests.

Supplementary Materials

Materials and Methods

Figs. S1 to S5

Tables S1 to S3

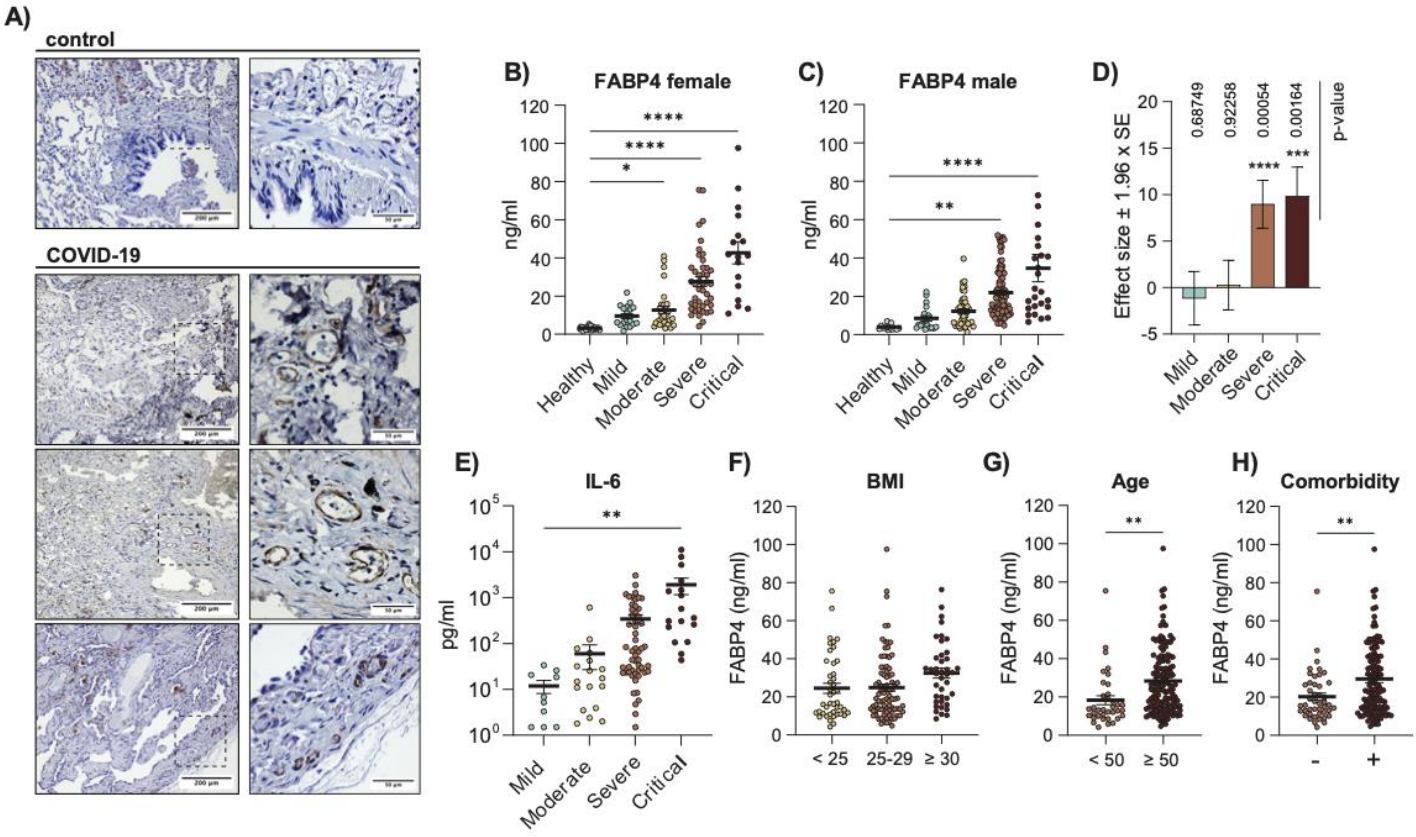

Fig. 1. FABP4 levels are increased in the lungs and circulation of COVID-19 patients. A) Immunohistochemical staining of lung biopsies of controls and COVID-19 patients, using anti-FABP4 antibody. B and C) Circulating FABP4 concentrations measured by from B) female and C) male COVID-19 patients and healthy controls, stratified based on disease severity. D) Effect size estimates and inference based on regression analysis of FABP4 concentration on COVID-19 severity while accounting for time of collection post symptom onset, age, gender, and BMI, using the linear mixed model to account for the patient-level random effects. The healthy controls were used as a reference group. p-values are calculated based on the Wald test. E) Circulating IL-6 levels in COVID-19 patients, stratified based on disease severity. Statistical analysis was performed using one-way ANOVA. E to G) Circulating FABP4 concentrations in severe and critical COVID-19 patients, stratified based on E) BMI, F) Age and G) the presence of comorbidities. B to G) Data are driven from the first patient cohort. Patients were sampled longitudinally, and the data represent the maximum measured concentration per patient. Statistical analysis was performed using a standard t-test. Data are shown as the mean ± s.e.m.

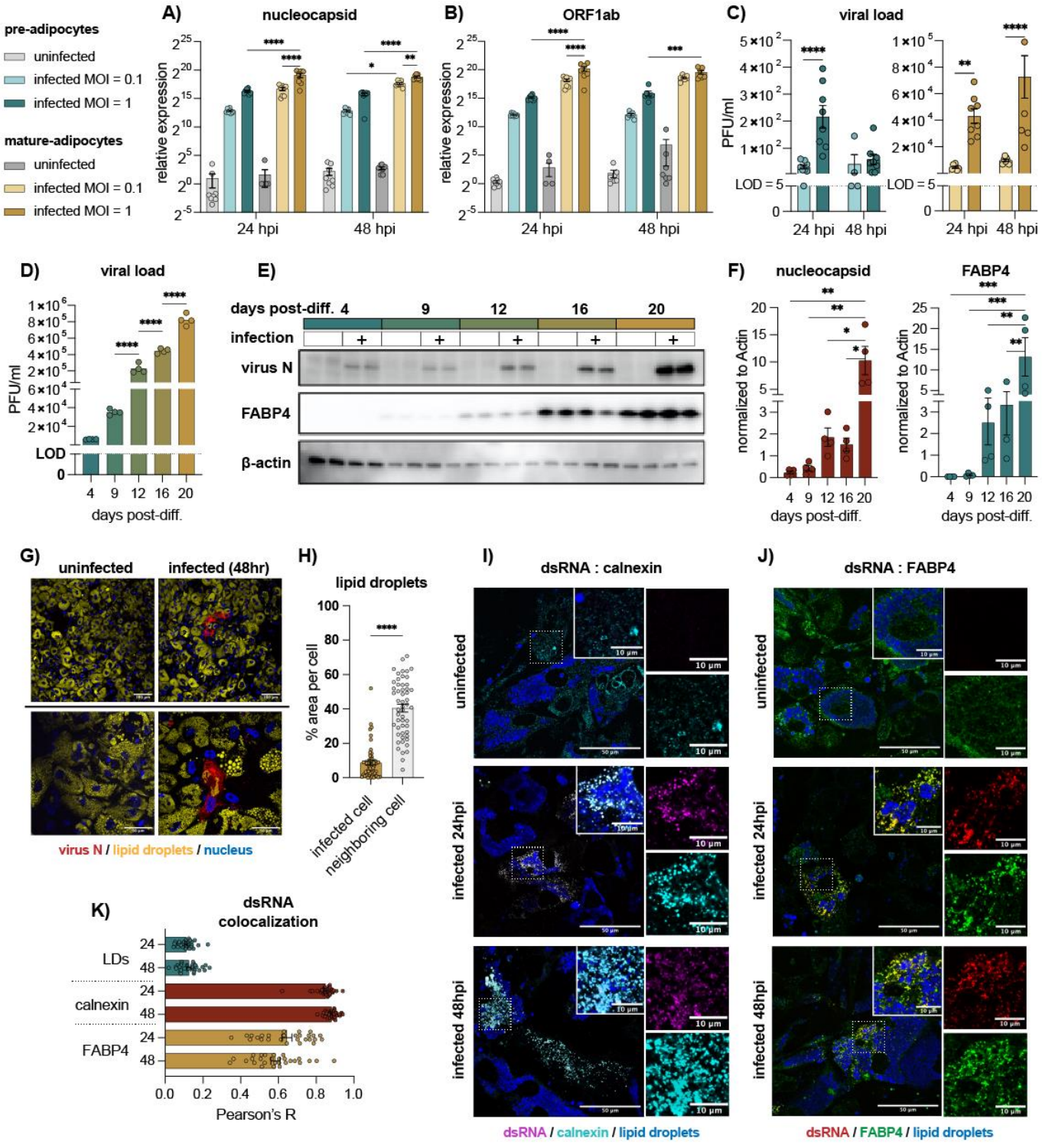

Fig. 2. FABP4 colocalizes with SARS-CoV2 replication organelles in human adipocyte cell lines. A to C) hTERT pre-adipocytes and mature adipocytes infected with SARS-CoV2 (WA1/2020) (MOI 0.1 or 1). Relative gene expression of the virus A) genomic (nucleocapsid) or B) sub-genomic RNA (ORF1ab) normalized to β-actin. C) Viral loads measured from supernatant using plaque assay. Data is pooled from two independent experiments, (n=8). Statistical analysis was performed using two-way ANOVA. D to F) Adipocytes were infected at 4, 9, 12, 16, and 20 days, post-differentiation (MOI 1). D) Viral loads

measured by plaque assay 48 hours post-infection. Data are representative of two independent experiments (n=4). Statistical analysis was performed using one-way ANOVA. E) Western blot of virus nucleocapsid, FABP4 and β-Actin from adipocyte lysates following infection. F) Quantification of the nucleocapsid and FABP4 band intensities normalized to β-actin. Data are representative of two independent experiments (n=4). Statistical analysis was done using two-way ANOVA. G) Confocal images of uninfected and infected mature hTERT cells (MOI 1) stained at 48h for SARS-CoV2 nucleocapsid (red), lipid droplet (yellow) and nuclear staining (Dapi, blue). Scale bar (upper panels: 100μm, lower panels: 50μm). H) Percent area of lipid droplets of infected cells and neighboring cells was quantified based on BODIPY (lipid droplet) signal. Data are pooled from two independent experiments, (n=6). Statistical analysis was performed using standard t-test. I and J) Infected hTERT cells (MOI 1), (n=3) fixed 24 and 48 hours, post-infection. I) Cells stained for dsRNA (red), calnexin (cyan) and lipid droplets (BODIPY, blue). Scale bar (50μm). J) dsRNA (red), FABP4 (green) and lipid droplets (blue) staining. Scale bar (50μm). Inlays represent magnified merged or single channel images of the areas indicated in I and J with a scale bar (10μm). K) Signal colocalization measure by Pearson's R between dsRNA with calnexin, FABP4 and lipid droplets. Data are shown as the mean ± s.e.m.

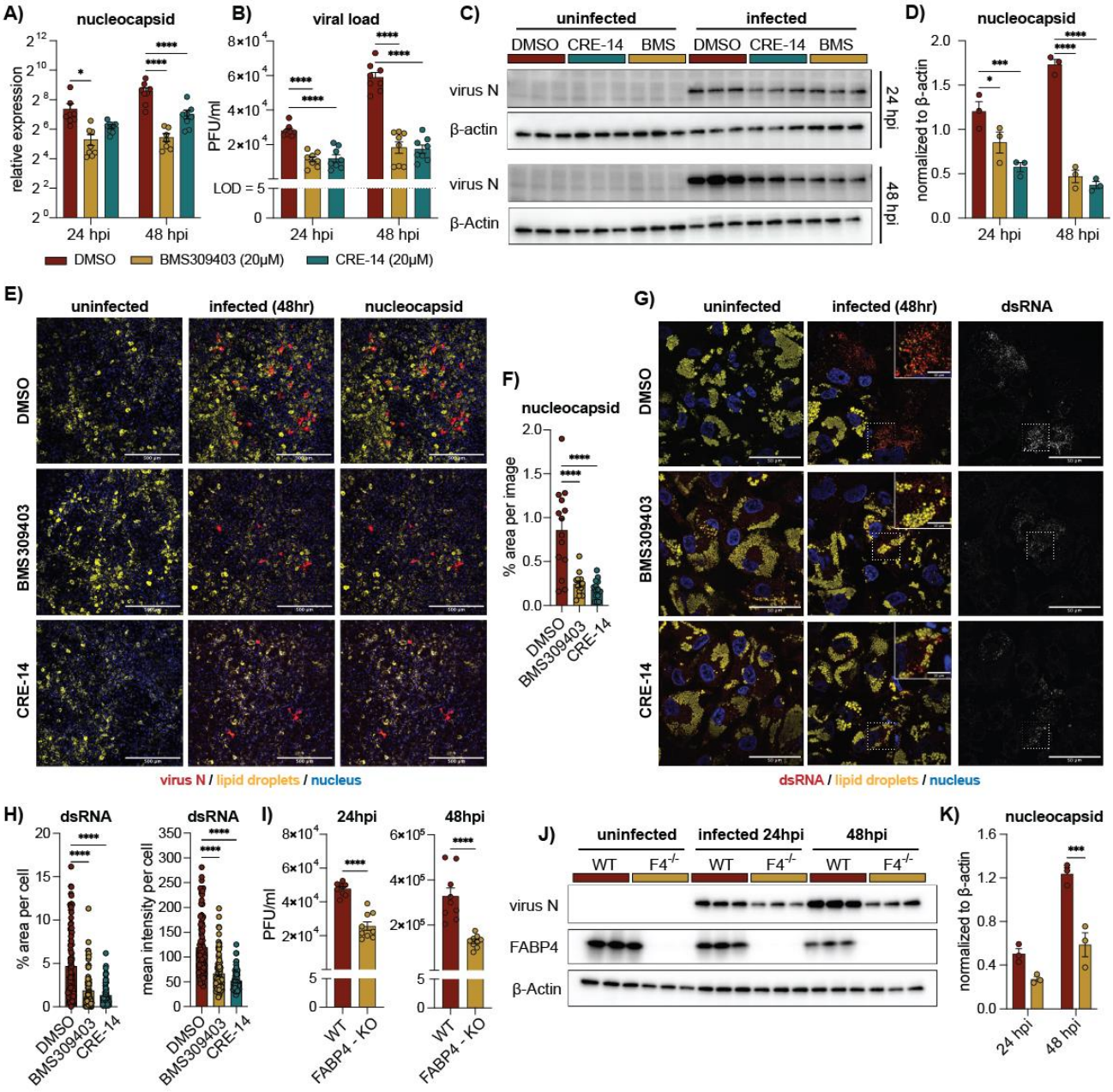

Fig. 3. FABP4 deficiency reduces virus titers and disrupts replication organelles formation in adipocytes. A – F) SARS-CoV2-infected mature hTERT adipocytes (MOI 1), treated with either DMSO or FABP4 inhibitors, BMS309403 (20μM) or CRE-14 (20μM). A) Relative RNA expression of SARS-CoV2 nucleocapsid, normalized to β-actin. Data pooled from two independent experiments, (n=8). B) Viral load measured by plaque assay. Pooled from two independent experiments, (n=8), representative of four independent experiments. Data were analyzed using two-way ANOVA. C) Western blot of nucleocapsid protein measured from cell lysates. D) Quantification of nucleocapsid band intensity normalized to β-actin. Data are representative of three independent experiments (n=3). E) Confocal images of adipocytes infected with SARS-CoV2 (MOI 1) then fixed 48 hours post-infection and stained for virus nucleocapsid (red), lipid droplets (BODIPY, yellow), and nuclei (DAPI, blue). (n=3) biological replicates. Scale bar (500μm). F) Percentage nucleocapsid positive area per image, with an average of 4-5 images per sample. G) Adipocytes infected with (MOI 3) and fixed 48 hours post-infection, then stained

for dsRNA (red), lipid droplets (BODIPY, yellow) and nuclei (DAPI, blue). (n=3) Scale bar (50μm). Inlays represent magnified images of the indicated area with a scale bar of (10 μm). H) Percentages of dsRNA positive area and mean fluorescence intensity per cell. (n=3) biological replicates. Statistical analysis was performed using one-way ANOVA. I to K) Infected wild type (WT) and *FABP4* knockout human adipocytes (MOI 1). I) Viral load measured by plaque assay from supernatants collected 24 and 48 hours post infected. Data are pooled from three independent experiments, (n=9). Statistical analysis was done using standard t-test. J) Western blot of nucleocapsid, FABP4 and β-actin proteins measured from cell lysates. K) Quantification of nucleocapsid band intensity normalized to β-actin. Data are representative of two independent experiments, (n=3). Data are shown as the mean ± s.e.m.

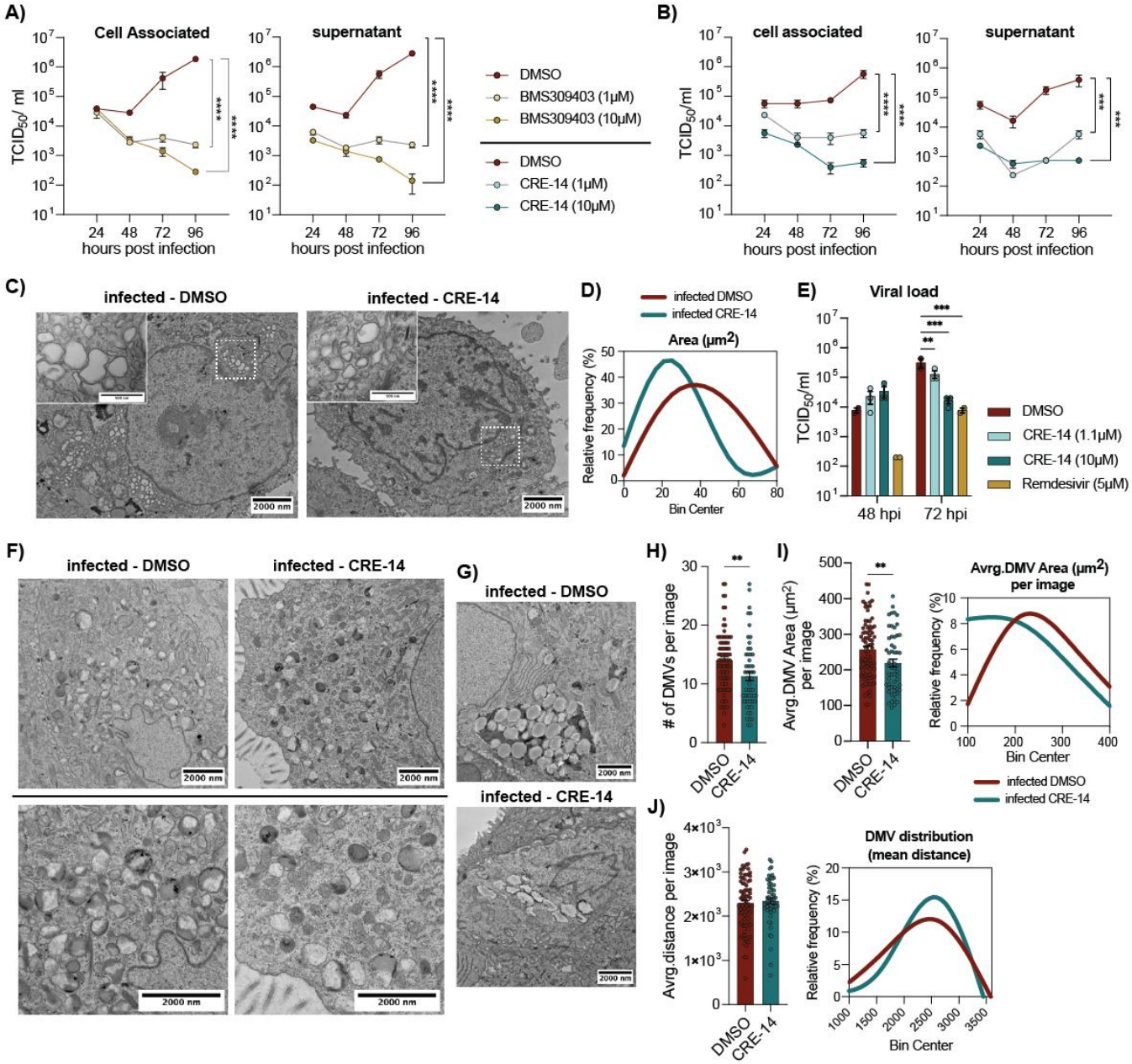

Fig. 4. Inhibition of FABP4 in bronchial epithelial cells disrupts virus replication organelles. A and B) Viral load measured by TCID50 from human bronchoepithelial (HBE) cells infected with SARS-CoV2 (strain Ank1, MOI 5) and treated with A) BMS309403 or B) CRE-14 at the indicated doses. Data are representative of two independent experiments, (n=3). Statistical analysis was performed using two-way ANOVA. C) Representative transmission electron microscopy (TEM) images of HBE cells 48 hours after infection with SARS-CoV2 (WA1/2020, MOI 1) and treatment with DMSO or CRE-14 (10µM). (n=3). D) Area of double membrane vesicles in infected HBE cells, determined from TEM images in C. Data displayed as the Fit Spline of the percent frequency distribution. E) Virus load measured by TCID50 of the apical wash of 3D airway epithelium cultures (MOI 0.1). Statistical analysis was performed using two-way ANOVA. (n=3). F to J) 3D reconstructed airway epithelium cultures were infected apically with 10^5 PFU of SARS-CoV2 (strain WA1/2020) then treated with either DMSO or CRE-14 through the basal layer. 24 hours after infection, the cells were fixed for EM and 3 sections per sample (n=2) were analyzed. F and G) Representative TEM images showing F) virus double-membrane vesicles (DMVs) and G) lipid droplets in control (DMSO) and inhibitor treated samples. H) Number of double membrane

vehicles and I) their average area per image. (n=2) biological replicates with 18-45 images per sample taken at an 8000X magnification. I) Frequency distribution of DMV area shown as a Fit Spline. J) The mean distance between DMVs within each image, calculated from the X, Y coordinates of each DMV and the percent frequency distribution shown as a fit spline. Statistical analyses were done using standard t-test. Data are shown as the mean ± s.e.m.

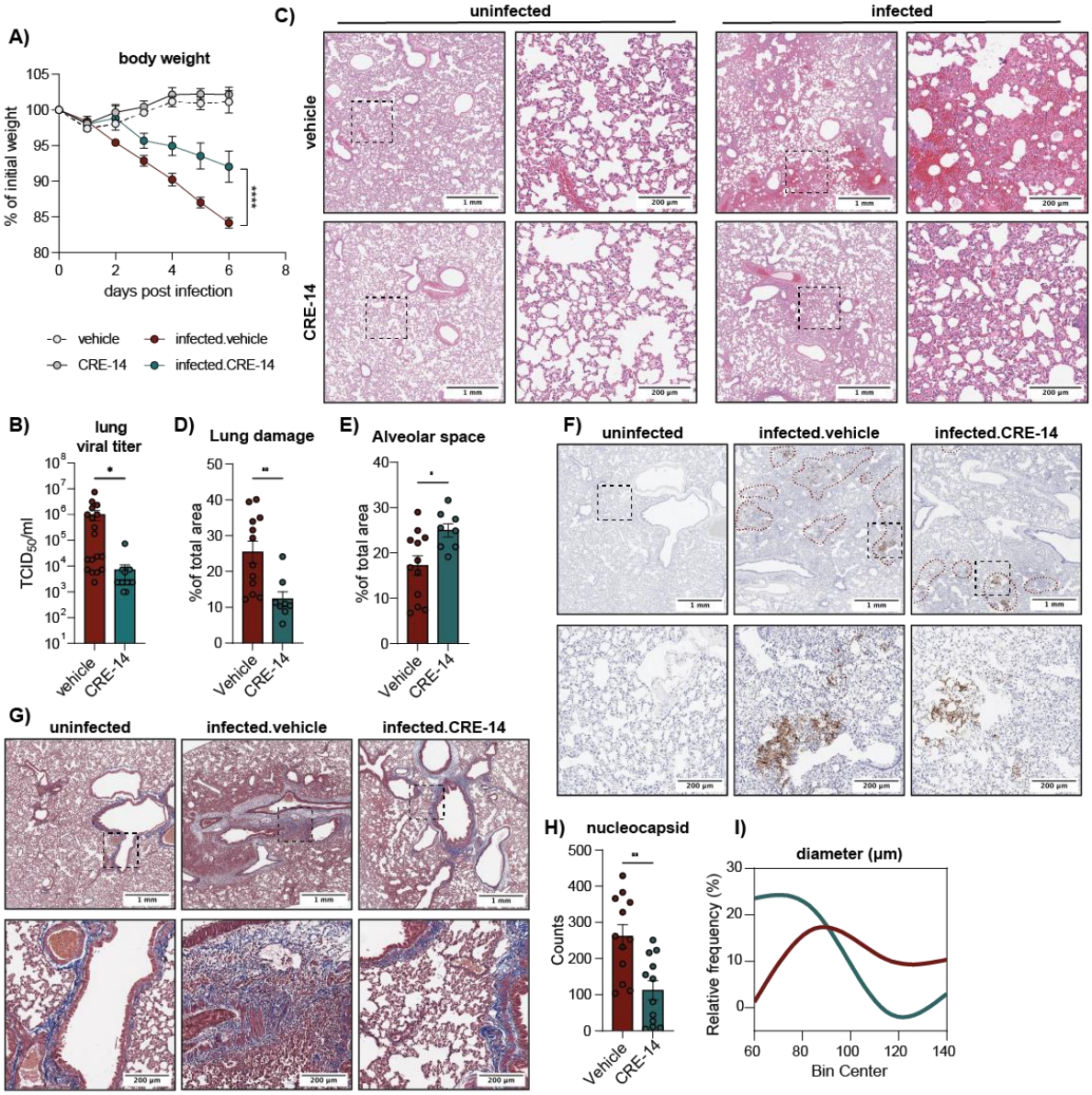

Fig. 5. FABP4 blockade limits virus replication and ameliorates pathology in infected hamsters. Syrian hamsters were infected intranasally with SARS-CoV2 (Ank1, 100 $TICD_{50}$) and treated daily with FABP4 inhibitor (15mg/kg, CRE-14) or vehicle. A) Percent of initial body weight. B) Lung viral titers measured by TCID50, pooled from three independent experiments. (n=18 and 17 for infected vehicle and CRE-14 respectively and n=6 for each of the uninfected groups). C) Representative H&E staining of the lungs of control and infected hamsters with or without inhibitor treatment. D and E) quantification of the D) area affected by damage and E) alveolar space, shown as percentage of total lung area. (n=5 with two lungs per animal). Statistical analysis was performed using standard t-test. F) Representative IHC of SARS-CoV2 nucleocapsid and G) Masson's trichrome straining of hamster lungs. H) Number of nucleocapsid positive areas, and I) frequency distribution of their diameter quantified from dataset represented in G. (n=4). Statistical analysis was performed using standard t-test. Data shows the mean ± s.e.m.